

This is the peer reviewed version of the following article:

Mycosporine-like Amino Acids and Other Phytochemicals Directly Detected by High-Resolution NMR on Klamath (*Aphanizomenon flos-aquae*) Blue-Green Algae / Righi, Valeria; Parenti, Francesca; Schenetti, Luisa; Mucci, Adele. - In: JOURNAL OF AGRICULTURAL AND FOOD CHEMISTRY. - ISSN 0021-8561. - STAMPA. - 64:35(2016), pp. 6708-6715. [10.1021/acs.jafc.6b02615]

Terms of use:

The terms and conditions for the reuse of this version of the manuscript are specified in the publishing policy. For all terms of use and more information see the publisher's website.

04/07/2024 03:19

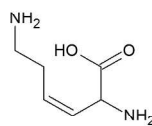
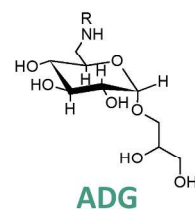
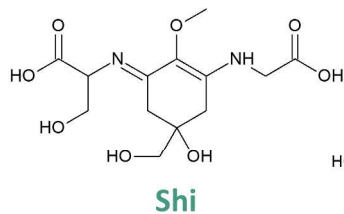
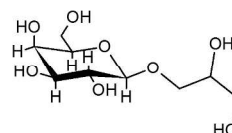
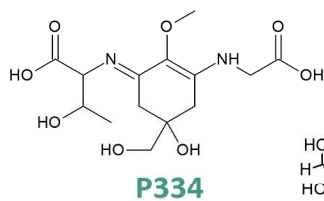
(Article begins on next page)

This document is confidential and is proprietary to the American Chemical Society and its authors. Do not copy or disclose without written permission. If you have received this item in error, notify the sender and delete all copies.

**Mycosporine-like amino acids and other phytochemicals
directly detected by high-resolution NMR on Klamath
(Aphanizomenon flos-aquae) blue-green algae**

Journal:	<i>Journal of Agricultural and Food Chemistry</i>
Manuscript ID	jf-2016-02615w.R1
Manuscript Type:	Article
Date Submitted by the Author:	n/a
Complete List of Authors:	Righi, Valeria; Università di Bologna, Dipartimento di Scienze per la Qualità della Vita Parenti, Francesca; Università di Modena e Reggio Emilia, Dipartimento di scienze Chimiche e Geologiche Schenetti, Luisa; Università di Modena e Reggio Emilia, Dipartimento di Scienze della Vita Mucci, Adele; Università di Modena e Reggio Emilia, Dipartimento di Scienze Chimiche e Geologiche

SCHOLARONE™
Manuscripts



For Table of Contents only

700x500mm (96 x 96 DPI)

1 **Mycosporine-like amino acids and other phytochemicals directly**
2 **detected by high-resolution NMR on Klamath (*Aphanizomenon flos-***
3 ***aquae*) blue-green algae**

4 Valeria Righi,^a Francesca Parenti,^b Luisa Schenetti,^c Adele Mucci^{b*}

5 ^aDipartimento di Scienze per la Qualità della Vita, Università di Bologna, via Corso d'Augusto 237, 47921
6 Rimini, Italy

7 ^bDipartimento di Scienze Chimiche e Geologiche, Università di Modena e Reggio Emilia, Via G. Campi 103,
8 41125 Modena, Italy

9 ^cDipartimento di Scienze della Vita, Università di Modena e Reggio Emilia, Via G. Campi 103, 41125
10 Modena, Italy

11

12

13 Corresponding author:

14 Prof. Adele Mucci

15 Dipartimento di Scienze Chimiche e Geologiche

16 Università di Modena e Reggio Emilia

17 Via G. Campi 103

18 41125 Modena

19 Italy

20 Tel.: +39 059 2058636; e-mail address: adele.mucci@unimore.it

21

22

23 **Abstract**

24 This study describes for the first time the use of the high-resolution nuclear magnetic resonance
25 (NMR) on Klamath (*Aphanizomenon flos-aquae*) blue-green algae directly on powder suspension. These
26 algae are considered a “superfood”, due to their complete nutritional profile that has proved to have
27 important therapeutic effects. The main advantage of NMR spectroscopy is that it permits the detection of a
28 number of metabolites all at once. Klamath algae metabolome revealed to be quite complex, and the most
29 peculiar phytochemicals that can be detected directly on algae by NMR are mycosporine-like amino acids,
30 (porphyra-334, **P334**; shinorine, **Shi**) and low molecular weight glycosides (glyceryl β -D-galactopyranoside,
31 **GalpG**; glyceryl 6-amino-6-deoxy- α -D-glucopyranoside, **ADG**) all compounds with a high nutraceutical
32 value. It is also noteworthy the presence of *cis*-3,4-DhLys that was revealed for the first time. This molecule
33 could be involved in the anticancer properties ascribed to AFA.

34

35

36 **Keywords:** *Aphanizomenon flos-aquae*, Nuclear Magnetic Resonance spectroscopy, Klamath algae,
37 mycosporine-like amino acids, glycosides, ESI-QTOF mass spectrometry

38

39

40

41

42 **INTRODUCTION**

43 *Aphanizomenon flos-aquae* (AFA) is a wild freshwater unicellular microalga that spontaneously grows in
44 copious amounts in Upper Klamath Lake (Klamath Falls, OR, USA) a volcanic lake with hot, deep and
45 mineral rich waters. The combination of water properties, clean air, and high intensity sunlight make the
46 unique ecosystem of Upper Klamath Lake the most perfect growing environment for this algae. AFA from
47 Klamath Lake attracts the interest of several scientists owing to its complete nutritional profile and
48 therapeutic properties and it is consumed as a nutrient food source and for its health-enhancing properties.¹⁻⁵

49 The microalga AFA Klamath exerts beneficial effects on various neurological dysfunctions,
50 including neurodegenerative diseases such as Alzheimer's and Parkinson's, multiple sclerosis, hyperactivity
51 and attention deficit disorders, autism, depression, memory deficit and mood disturbances.^{1,6-12}

52 AFA algae are prokaryote cells (cyanobacteria) which are capable to implement the photosynthesis
53 process despite their simple structure. Their green-blue colour is due to the presence of phycobiliproteins, a
54 family of highly soluble and reasonably stable fluorescent proteins containing a covalently linked
55 tetrapyrrole prosthetic group (phycocyanobiline). Phycocyanobilines are pigments that collect light and
56 convey it (through fluorescence resonance energy transfer) to a pair of chlorophyll molecules located in the
57 photosynthetic reaction center of the cyanobacteria starting the photosynthetic process. AFA is an important
58 source of the blue photosynthetic pigment phycocyanin, (a complex between the pigment phycocyanobiline
59 with phycobiliproteins) which has been described as a strong antioxidant¹³⁻¹⁵ and anti-inflammatory^{16,17}
60 natural compound, as evidenced by *in vitro* and *in vivo* studies on phycocyanin from the cyanophyta
61 *Spirulina platensis*. In addition, Klamath is an important source of β -phenylethylamine, a sort of natural
62 endogenous amphetamine-like compound that is able to modulate mood.

63 Recently, attention has also been devoted to the composition of AFA which appear to contain
64 mycosporine-like amino acids (MAAs), in particular porphyra-334 (P334) and shinorine (Shi), as
65 monoamine oxidase (MAO) inhibitors, which seem present in relatively high concentration in AFA Klamath
66 microalgae.^{5,18,19} These are structurally simple water-soluble molecules, with a molecular weight of 300-350
67 Da, that easily cross the blood-brain barrier, and then are able to express their MAO-B inhibitory potential in
68 the area where it is mostly needed, the brain. Moreover, MAA are reported to be antioxidant, UV-protective
69 and wound healing agents.²⁰

70 For the chemical analysis of these biologically active compounds, different conventional techniques
71 are used: extraction, chromatography,²¹⁻²³ and UV-Vis and IR.^{24,25} Each of these chemical analysis techniques
72 allows identifying only one or few classes of chemical compounds at a time, and requires a sample
73 pretreatment.

74 In this work, we present, for the first time to the best of our knowledge, the application of high-
75 resolution nuclear magnetic resonance (NMR) spectroscopy to the study of deuterated water (D₂O)
76 suspension of commercially available Klamath powder for the detection of several metabolites all at once.
77 This approach has the advantage of avoiding any sample pretreatment that can alter algae composition. The
78 NMR spectra obtained are very complex, and this work does not expect to be exhaustive in describing the
79 metabolome of AFA but, despite the evident spectral overcrowding, we will show that P334, and at a minor
80 extent Shi can be detected directly on the water suspension, without the need of extraction. Together with
81 these MAAs, another two molecules were recognised, glyceryl β-D-galactopyranoside (GalpG) and *cis*-3,4-
82 dehydrolysine (DhLys) among other minor species. These findings were checked with Electrospray
83 Ionization Quadrupole-Time-of-Flight mass spectrometry (ESI-QTOF-MS) and low-energy Collision-
84 Induced Dissociation tandem mass spectrometry (CID MS/MS).

85

86 Scheme 1 near here

87

88 MATERIALS AND METHODS

89 **Sample preparation.** A suspension of dry powder of alga klamath (Farmalabor S.r.l, Canosa di Puglia, Italy,
90 batch: P1001594-000), 40 mg in 700 μL D₂O 99.8%, was sonicated at 25 °C for 1 h and directly used for
91 NMR measurements. Samples for ESI-QTOF-MS measurements were obtained by suspending algae in
92 deionized water (1 mg in 1 mL), sonicated at 25 °C for 1 h, centrifuged at 13000 rpm, for 10 min and the
93 supernatants, diluted 1:30 in deionized water, were directly analysed. All measurements were performed at
94 autogenous pH (5.6).

95 **NMR experiments.** NMR spectra were recorded with a AVANCE III HD 600 spectrometer (Bruker)
96 equipped with a CryoProbe BBO H&F 5 mm (operating at 600.13 and 150.90 MHz for proton and carbon,
97 respectively) at 300 K. Ala CH₃ signal (at 1.47 and 19.0 ppm, for proton and carbon, respectively, see Table
98 S1) was used as internal reference for ¹H and ¹³C chemical shifts. 1D proton spectra were acquired using the

99 standard zgcppr sequence with 2.5 s water presaturation during relaxation delay, 12 kHz spectral width, 64k
100 data points, 64 scans. 2D COSY spectra were acquired using a standard pulse sequence (cosygpprqf) and 1 s
101 water presaturation during relaxation delay, 7 kHz spectral width, 4k data points, 16 scans per increment, 512
102 increments. 2D TOCSY spectra were acquired using a standard pulse sequence (mlevgpph19) and 0.5 s
103 relaxation delay, 100 ms mixing (spin-lock) time, 7 kHz spectral width, 4k data points, 32 scans per
104 increment, 512 increments. 2D NOESY and ROESY spectra were acquired using standard pulse sequences
105 (noesygpph19, roesyphpr) and 1 s relaxation delay, 500 and 250 ms mixing time, respectively, 7.2 kHz
106 spectral width, 4k data points, 24 scans per increment, 512 increments. 2D HSQC edited spectra were
107 acquired using a standard pulse sequence echo-antiecho phase sensitive (hsqcedetgppsp.3) and 0.5 s relaxation
108 delay, 1.725 ms evolution time, 7 kHz spectral width in f_2 , 4k data points, 96 scans per increment, 25 kHz
109 spectral width in f_1 , 320 increments. 2D HMBC spectra were acquired using a standard pulse sequence
110 (hmbcgplpndqf) with 0.5 s relaxation delay, 3.4 ms low-pass J filter and 50 ms evolution time, 7 kHz spectral
111 width in f_2 , 4k data points, 128 scans per increment, 30 kHz spectral width in f_1 , 300 increments. HSQC-
112 TOCSY experiment was acquired using a standard pulse sequence (hsqcdiedetgpsisp.1) and 0.5 s relaxation
113 delay, 1.725 ms evolution time, 110 ms spin-lock, 8 kHz spectral width in f_2 , 2k data points, 96 scans per
114 increment, 23 kHz spectral width in f_1 , 280 increments.

115 **ESI-QTOF experiments.** Positive and negative ion high-resolution ESI-QTOF-MS and low-energy CID
116 MS/MS spectra were acquired with an 6520 Accurate-Mass QTOF LC/MS (Agilent Technologies) coupled
117 with a HPLC Agilent Series 1200 equipped with a Zorbax SB-C18 column, 100x2.1mm ID, 3.5 μ m particle
118 size (Agilent). Eluents were acetonitrile (eluent A) and H₂O with 0.2% ammonium formiate (eluent B).
119 Chromatographic runs were performed using a gradient of eluent A [starting from 1% (1 min) to 40% (in 20
120 min) to 100% (in 10 min)]. The solvent flow rate was 0.3 ml/min, the temperature kept at 25 °C and the
121 injector volume selected was 2 μ l. Total ion current (TIC) chromatograms were acquired in the mass range
122 between 50 and 1700 m/z. Nitrogen was used as collision gas in MS/MS experiments. Nitrogen nebulizer
123 pressure was 30 psi, nitrogen dry gas flow and temperature were 9 L/min and 350 °C, respectively, and
124 capillary voltage was 3.5 kV. Exact masses were checked, in order to verify the correspondence to the
125 proposed molecular formulas, within 10 ppm that is the maximum estimated mass error. The isotopic peak
126 intensity ratios of molecular species were checked with the “generate-formula-from-peaks” tool of
127 Qualitative Analysis (Version B.04.00, Agilent Technologies, Inc. 2011).

128

129 **RESULTS AND DISCUSSION**

130 Since powder alga Klamath forms suspensions in D₂O, we first evaluated the use of High Resolution Magic
131 Angle Spinning (HR-MAS) which is an NMR technique that bridges the divide between high-resolution
132 NMR in solution and solid-state NMR. HR-MAS is the election NMR technique when semisolid samples,
133 such as vegetable tissues, are investigated. In fact, it does not need of any pretreatment, extraction and
134 separation, and the signals from polar and apolar fractions are detected simultaneously.^{26,27} Nevertheless,
135 when the NMR AFA spectra obtained with HR-MAS probe were compared to those acquired with probes for
136 liquids (AFA suspended into standard 5 mm NMR tubes), we did not observe any difference (Fig. S1).
137 Hence, we decided to carry out this investigation directly in this last way, i.e. on suspensions of dry powder
138 of alga Klamath in D₂O. The signals thus observed are due to molecules in solution, and the little suspended
139 material does not affect negatively spectral resolution.

140 The water presaturated ¹H NMR spectrum of alga Klamath suspension is reported in Fig. 1. It is a very
141 complex spectrum, dominated by the acetate signal at 1.93 ppm, then by signals within the carbohydrate
142 region (5.5-3 ppm), the majority of which belong to high molecular weight species, that are in the negative
143 NOE regime.²⁸

144 Resonances due to aliphatic amino acids at low ppm are also clearly detected. Lower signals are found in
145 the anomeric/ethylenic region and very low resonances in the aromatic one. An attempt to disentangle, at
146 least partially, this heavily overlapped pattern was done through 2D homonuclear and heteronuclear spectra.
147 COSY, TOCSY, NOESY, HSQC, HSQC-TOCSY and HMBC spectra were acquired, analysed and a number
148 of metabolites was identified. The results are reported in Tables 1 and S1.

149 Some of the detected metabolites (alanine, Ala, and other aliphatic amino acids, acetate, Ac, lactate, Lac,
150 aspartate, Asp, glutamate, Glu, glutamine, Gln, threonine, Thr, glucose, Glc, etc.) are quite common in
151 natural matrixes and their signals can be readily interpreted and assigned. Nevertheless, in the case of alga
152 Klamath a group of signals in the region 2.6 - 2.9 ppm, partially overlapped to those of CH₂-β of Asp (H/C
153 correlations: 2.82,2.68/39.7), attracted our attention. These resonances are due to two CH₂ with
154 diastereotopic protons (H/C correlations: 2.89,2.74/36.1 ppm and 2.82,2.75/35.8 ppm, Fig. 2), that give two
155 AB systems. They also give H,C long range correlations in HMBC spectrum (not shown) with carbons at
156 73.8, 128.0, 161.8 and 163.3 ppm, that allow to assembly the MAA skeleton (Scheme 1). This hypothesis

157 was confirmed by other H,C long range and H,H NOE and ROE correlations (Fig. 3, Table 1), and allow to
158 identify the presence of P334. P334 should be in its protonated form, for both H-11 and H-8 give correlations
159 with NH protons in TOCSY experiment. These data compare well with those reported in the literature.^{18,29}
160 Moreover, very close to P334 major signals, minor resonances were found at 2.92 and 2.77 ppm. They show
161 clear ROESY cross peaks with protons at 4.34 and 3.57 ppm (Fig. 3). Signal at 4.34 derives from a methine
162 proton (C 63.3 ppm) that correlates in COSY spectrum with methylene signals at 3.92 and 3.99 ppm (C 65.3
163 ppm) and with carbons at 177.5 and 161.9 ppm in the HSQC spectrum. This second set of minor signals was
164 assigned to Shi, the other resonances of which overlap those of P334. Also in this case the spectral data
165 parallel those reported in the literature for Shi methyl ester.³⁰

166 Due to the high overlapping of P334 and Shi signals in the ¹H NMR spectrum, an estimate of the relative
167 P334/Shi molar ratio of about 3:1 is better obtained, in the hypothesis of a very similar conformation, from
168 the integrals of the cross peaks between CH₂-4 and CH-11 in the ROESY spectrum. Alternatively, in the
169 hypothesis of similar ¹J_{H-C} coupling values for the C,H-11 pair in both compounds, the P334/Shi molar ratio
170 can be estimated by the HSQC C,H-11 correlations (at 4.06/67.3 ppm for P334 and at 4.34/63.3 ppm for Shi)
171 as 2.3:1. However, in this case, the volume of P334 C,H-11 cross peak is underestimated, due to its proximity
172 to a CH₂ correlation of opposite sign.

173 The presence of both P334 and Shi was confirmed by ESI-MS and low-energy CID MS/MS spectra (see
174 ESI-QTOF mass analysis section).

175 Figure 1 near here

176 Figure 2 near here

177 Figure 3 near here

178

179 Another group of interesting and intense correlations was distinguished in the HSQC carbohydrate region.
180 The most characteristic signals are the β-D-galactose doublet at 4.40 ppm (bound to C at 105.8 ppm that
181 indicates the presence of a β-glycosidic linkage), and two methylene groups, with diastereotopic protons, and
182 H,C correlations that are found at 3.76,3.91/73.7 ppm and 3.60,3.66/65.3 ppm. Starting from 4.40 doublet, it
183 is possible to derive a β-galactose spin system, through COSY and TOCSY correlations, up to H-4 at 3.92
184 ppm, due to the low J coupling H-4,H-5 that lowers the efficiency of coherence transfer. Nevertheless, H-4
185 correlates with C-6, C-5, C-2 and C-3 in HMBC spectrum and these correlations permit to reconstruct the

186 galactopyranosyl unit. Inter-residue ROE correlations between H-1 and 3.76,3.91 methylene signals allow
187 GalpG (Fig. 2) to be recognized, and HSQC-TOCSY spectrum (Fig.S2a) confirms that 3.76,3.91 protons
188 belong to the same spin system to which 3.60,3.66 protons belong, too. GalpG gives also rise to the highest
189 signals in ^{13}C spectrum and its presence was confirmed by ESI-QTOF-MS results (see ESI-QTOF mass
190 analysis section). This seems to us a quite peculiar finding, since α -D-galactopyranosyl glycerols are usually
191 found in algae³¹ and GalpG appears to be a glycoside that characterizes AFA metabolome.

192 A minor doublet at 4.43 ppm (bound to C at 105.8 ppm) indicates the presence of another minor β -D-
193 galactoside, the spin system of which was only partially identified. Similarly, other low correlations due to
194 glycosidic units were found (Table S1). The presence of GalpG, and similar water soluble molecules could be
195 related to different types of glycolipids,³² that have significant anti-tumor activities towards different
196 targets.

197 Two interesting spin systems were also highlighted by TOCSY (Fig. 4).

198  Figure 4 near here

199 The former recalls the spectral features of a 6-amino-6-deoxy- α -D-glucopyranoside. The starting point is a
200 methylene with diastereotopic protons at 3.07 and 3.38 ppm (C at 54.9 ppm), the correlations of which (in
201 COSY, TOCSY and HSQC spectra) allow to gather a spin system formed by oxygenated methylenes (H/C
202 pairs: 4.05/70.9 3.26/75.4, 3.73/75.7, 3.58/74.4,) terminating with an α -anomeric proton at 4.89 ppm (C at
203 101.1 ppm). The HSQC-TOCSY experiment (Fig.s S2b and S2d) confirms the assignments. The anomeric
204 proton at 4.89 ppm correlates, in the HMBC spectrum, with a carbon at 71.7 ppm, not belonging to the
205 amino sugar ring, and gives ROE peaks with protons at 3.58 ppm (its vicinal one) and 3.45, 3.94 ppm. These
206 last two protons belong to a methylene group (the carbon of which resonates at 71.7 ppm, Fig. S3a) that
207 gives HMBC correlations with carbons at 101.1 (bound to the proton resonating at 4.89 ppm), 73.6
208 (methyne) and 65.5 ppm (methylene). No unambiguous one-bond proton-carbon correlation (in the HSQC
209 spectrum) for carbons at 73.6 and 65.5 ppm. These findings point to a glyceryl 6-amino-6-deoxy- α -D-
210 glucopyranoside (ADG). The proton (shifted by 0.3 – 0.5 ppm due to the different solvents employed) and
211 carbon chemical shifts (within 0-3 ppm) parallel those reported for the 6-amino-6-deoxy ring of ishigoside, a
212 glyceroglycolipid isolated from the Brown Alga *Ishige okamurae*, with radical scavenging properties.³³ This
213 seems to us another interesting finding, for it indicates the presence of glycerol 6-amino-6-deoxy glucosides
214 in AFA. Nevertheless, we did not identify, through ESI-QTOF mass analysis, adducts related to ADG (see

215 ESI-QTOF mass analysis section), hence we cannot exclude a further functionalization of this moiety at the
216 amino group.

217 The second spin system is even more unusual and corresponds to DhLys. This spin system can be
218 identified starting for instance from the doublet at 4.59 ppm (C at 54.7 ppm) which gives a COSY cross-peak
219 with a triplet at 5.66 ppm and TOCSY cross peaks with protons at 5.88, 5.66, 2.58, 2.66, 3.13 and 3.19 ppm.
220 The last four belong to methylenes group, the carbons of which are found at 28.2 and 41.4 ppm, respectively.
221 The presence of a double bond on the backbone of the fragment is confirmed by the chemical shifts of
222 carbons bound to 5.66 and 5.88 ppm protons (128.1 and 135.1 ppm, respectively) and the *cis*- configuration
223 of the double bond is derived by the coupling constant (about 10 Hz) between the two ethylenic protons, and
224 a clear ROE between 4.59 ppm and 2.58, 2.66 ppm signals. This spectral picture is confirmed by HSQC-
225 TOCSY correlations (Fig. S3c). No inter-residue ROEs were detected for DhLys and, in this case, a mass
226 peak corresponding to the protonated molecule $[M+H]^+$ was found in ESI-QTOF spectra, confirming the
227 presence of this molecule. Nevertheless, DhLys appears to be quite puzzling, for usually *trans*-3,4-DhLys
228 moiety is found in important anticancer bioactive compounds, such as syringolin A (SylA). Syl A has been
229 identified as a virulence factor, which irreversibly inhibits the 20S proteasome through a covalent
230 mechanism.³⁴ Proteasome inhibitors, such as the clinically-used anticancer agent bortezomib, represent a
231 powerful class of chemotherapeutics.³⁵ Syls are a family (Syl A-F) of natural products formed by twelve-
232 membered macrolactams produced by strains of *Pseudomonas syringae*. The targeted search of protonated
233 molecule or other adducts of Syls A, D and F (those containing *trans*-DhLys) within ESI-QTOF mass
234 spectral data did not give any result. Hence, we cannot derive a correlation between the presence of *cis*-3,4-
235 DhLys and Syls in AFA.

236 A final comment is deserved to the aromatic region of the proton spectrum (Fig. 1), characterized by
237 resonances mainly due to nucleobase derivatives (Table S1). Signals from alkylsubstituted phenyl rings were
238 found, as confirmed by the HSQC experiment, that displays correlations between proton (7.4 ÷ 7.2 ppm) and
239 carbon (133 ÷ 130 ppm) signals. Nevertheless, we cannot relate these resonances to free phenylethylamine,
240 because its aliphatic signals were not clearly detected.

241 High performance liquid chromatography ESI-QTOF-MS was employed, operating both in positive and
242 negative ionization mode, to confirm the presence of the metabolites detected through NMR analysis. The
243 ESI-QTOF-MS (positive ion mode) gave a very complex total ion current chromatogram. The metabolites

244 GalpG, Shi and P334 eluted within the first two minutes and gave the highest contribution to the total ion
245 current to peaks at 1.5, 1.8 and 2.0 min. DhLys peak co-eluted with other ions at 1.3 min. DhLys, P334 and
246 Shi were detected as the protonated molecule $[M+H]^+$, whereas GalpG was detected as a mixture of the
247 protonated molecule $[M+H]^+$ and ammonium adduct $[M+NH_4]^+$.
248 In addition, in ESI-QTOF-MS negative ion mode experiments the metabolites were detected as $[M-H]^-$ ions,
249 whereas GalpG was also detected as formiate adduct $[M+HCOO]^-$ at m/z 299.

250 Low-energy CID MS/MS spectra of Shi and P334 (Fig. S4) parallel those reported by other
251 authors,³⁶ whereas GalpG CID spectrum in negative mode (Fig. S5) is similar to that reported for its α -
252 isomer by Chen et al..³⁷ The formulae that best fit the experimental isotopic peak intensity ratios of molecular
253 species were $C_{14}H_{22}N_2O_8$ and $C_{13}H_{20}N_2O_8$ for P334 and Shi, respectively.

254 In the case of GalpG, the isotopic cluster of the protonated molecule and of the ammonium adduct
255 suffer from peak overlapping with other species in all the MS spectra acquired. Hence, we checked the
256 isotopic peak intensity ratio of the product ion $[M-H]^-$ cluster at m/z 253, obtained from the product ion scan
257 of the formiate adduct $[M+HCOO]^-$ at m/z 299. The formula that best fits experimental intensities is $C_9H_{18}O_8$.
258 We were not able to check the isotopic cluster intensities of m/z 145 DhLys peak, for it suffers from severe
259 overlapping in all MS spectra and we did not find other molecular species other than $[M+H]^+$ and $[M-H]^-$
260 (Fig. S6).

261 As for ADG, we did not come to an unambiguous structural assignment through MS/MS spectra. We
262 searched the product ion scans for neutral losses of amino sugars (m/z 179) or of their dehydrated forms (m/z
263 161) and for product ions corresponding to protonated amino sugars (m/z 180) or protonated dehydrated
264 amino sugars (m/z 162). A possible species containing the 6-amino-6-deoxy- α -D-glucopyranosyl fragment
265 could be the m/z 455 ion (Fig. S7) that displays a m/z 179 neutral loss and shows product ions at m/z 162
266 and 180. The remaining ions, in particular those at m/z 84, 126, 138, 144, 168, 186 and 276, are the same
267 reported for the fragmentation of *N*-acetyl muramic acid. Our data suggest that m/z 455 ion could derive
268 from *N*-acetyl muramic acid, or an isomer of it, bound to an amino sugar. *N*-acetyl muramic acid is usually
269 bound to *N*-acetyl glucosamine in bacterial cells, and it has been reported that cell walls of blue-green algae
270 possess a mucopolymer similar to that of bacterial cell walls.³⁸ Thus, we hypothesize that ADG could be
271 involved in the structure of such a mucopolymer.

272 Summarizing, we showed that high-resolution NMR spectroscopy applied to AFA powder
273 suspensions reveals a very complex metabolic profile. Resonances from small metabolites, overlapped to a
274 background due to signals coming from high molecular weight polysaccharides, were detected. Apart from
275 free and bound amino acids and monosaccharides, the most interesting metabolites found are two MAAs, *i.e.*
276 P334 and Shi, two glycopyranosides, *i.e.* GalpG, and ADG, and *cis*-3,4-DhLys. All these molecules possess
277 known nutraceutical properties and high biological activity. The presence of *cis*-3,4-DhLys was revealed for
278 the first time, even though we were not able to find a direct connection to Syla production.

279 NMR findings were checked by ESI-QTOF-MS that confirmed most of them, leaving the complete
280 structure of the ADG-derivative still an open question.

281 Although this study proves the value of the application of NMR spectroscopy directly on complex
282 mixtures and it supports the use of NMR to monitor valuable metabolites, such as P334 and Shi, directly of
283 AFA powder suspensions, further investigations are necessary to gain a deeper insight into the very complex
284 AFA metabolome.

285

286 **ABBREVIATIONS**

287 Ac, acetate; ADG, glyceryl 6-amino-6-deoxy- α -D-glucopyranoside; AFA, *Aphanizomenon flos-aquae*; Ala,
288 alanine; Asp, aspartate; CID MS/MS, low-energy Collision-Induced Dissociation tandem mass spectrometry;
289 COSY, COrrrelation Spectroscopy; DhLys, dehydrolysine; ESI, Electrospray Ionization; GalpG, glyceryl β -D-
290 galactopyranoside; Glc, glucose; Gln, glutamine; Glu, glutamate; HMBC, Heteronuclear Multiple Bond
291 Correlation; HR-MAS, High Resolution Magic Angle Spinning; HSQC, Heteronuclear Single Quantum
292 Coherence; Lac, lactate; MAAs, mycosporine-like amino acids; MAO, monoamine oxidase; MS, mass
293 spectrometry; NMR, Nuclear Magnetic Resonance; NOESY, Nuclear Overhauser Effect Spectroscopy;
294 P334, porphyra-334; QTOF, Quadrupole-Time-of-Flight; ROESY, Rotating Overhauser Effect Spectroscopy;
295 Shi, shinorine; Syl, syringolin; Thr, threonine; TOCSY, TOtal Correlation Spectroscopy.

296

297 **ACKNOWLEDGEMENTS**

298 Fondazione Cassa di Risparmio di Modena and Centro Interdipartimentale Grandi Strumenti of the
299 University of Modena and Reggio Emilia are greatly acknowledged for financial support in the acquisition of
300 the Bruker Avance III HD 600 Spectrometer.

301

302 **SUPPORTING INFORMATION**

303 SI contains Figures reporting selected regions of HSQC-TOCSY, HSQC spectra, low-energy CID MS/MS
304 spectra and a Table with further NMR data for metabolites found in AFA.

305

306

307 REFERENCES

- 308 (1) Baroni, L.; Scoglio, S.; Benedetti, S.; Bonetto, C.; Pagliarani, S.; Benedetti, Y.; Rocchi, M.; Canestrari,
309 F. Effect of a Klamath algae product ("AFA-B12") on blood levels of vitamin B12 and homocysteine in
310 vegan subjects: a pilot study. *Int. J. Vitam. Nutr. Res.* **2009**, *79*, 117–123.
- 311 (2) Hart, A. N.; Zaske, L. A.; Patterson, K. M.; Drapeau, C.; Jensen G. S. Natural killer cell activation and
312 modulation of chemokine receptor profile in vitro by an extract from the cyanophyta *Aphanizomenon*
313 *flos-aquae*. *J. Med. Food* **2007**, *10*, 435–441.
- 314 (3) Pugh, N.; Pasco, D.S. Characterization of human monocyte activation by a hydrosoluble preparation of
315 *Aphanizomenon flos-aquae*. *Phytomedicine* **2001**, *8*, 445–453.
- 316 (4) Scoglio, S.; Benedetti, S.; Canino, C.; Santagni, S.; Rattighieri, E.; Chierchia, E.; Canestrari, F.;
317 Genazzani, D. A. Effect of a 2-month treatment with Klammin®, a Klamath algae extract, on the general
318 well-being, antioxidant profile and oxidative status of postmenopausal women. *Gynecol. Endocr.* **2009**,
319 *25*, 235–240.
- 320 (5) Scoglio, S.; Benedetti, Y.; Benvenuti, F.; Battistelli, S.; Canestrari, F.; Benedetti, S. Selective
321 monoamine oxidase B inhibition by an *Aphanizomenon flos-aquae* extract and by its constitutive active
322 principles phycocyanin and mycosporine-like amino acids. *Phytomedicine* **2014**, *21*, 992–997.
- 323 (6) Benedetti, S.; Benvenuti F.; Pagliarani S.; Francogli S.; Scoglio, S.; Canestrari, F. Antioxidant properties
324 of a novel phycocyanin extract from the blue-green alga *Aphanizomenon flos-aquae*. *Life Sci.* **2004**, *75*,
325 2353–2362.
- 326 (7) Benedetti, S.; Benvenuti, F.; Scoglio, S.; Canestrari, F. Oxygen radical absorbance capacity of
327 phycocyanin and phycocyanobilin from the food supplement *Aphanizomenon flos-aquae*. *J. Med. Food*
328 **2010**, *13*, 223–227.
- 329 (8) Gilroy, D. J.; Kauffman, K. W.; Hall, R. A.; Huang, X.; Chu F. S. Assessing potential health risks from
330 microcystin toxins in blue-green algae dietary supplements. *Environ. Health Persp.* **2000**, *108*, 435–439.
- 331 (9) Kusaga, A. Decreased beta-phenylethylamine in urine of children with attention deficit hyperactivity
332 disorder and autistic disorder. *No To Hattatsu* **2002**, *34*, 243–248.
- 333 (10) Kusaga, A.; Yamashita, Y.; Koeda, T.; Hiratani, M.; Kaneko, M.; Yamada, S.; Matsuishi, T. Increased
334 urine phenylethylamine after methylphenidate treatment in children with ADHD. *Ann. Neurol.* **2002**, *52*,
335 372–374.

- 336 (11) Sedriep, S.; Xia, X.; Marotta, F.; Zhou, L.; Yadav, H.; Yang, H.; Soresi, V.; Catanzaro, R.; Zhong, K.;
337 Polimeni, A.; Chui, D. H. Beneficial nutraceutical modulation of cerebral erythropoietin expression and
338 oxidative stress: an experimental study. *J. Biol. Reg. Homeos. Ag.* **2011**, *25*, 187–194.
- 339 (12) Shytle, D. R.; Tan, J.; Ehrhart, J.; Smith, A. J.; Sanberg, C. D.; Sanberg, P. R.; Anderson, J.;
340 Bickford, P. C. Effects of blue-green algae extracts on the proliferation of human adult stem cells in
341 vitro: a preliminary study. *Med. Sci. Monit.* **2010**, *16*, 1–5.
- 342 (13) Bhat, V. B.; Madyastha, K. M. C-phycoyanin: a potent peroxy radical scavenger in vivo and in
343 vitro. *Biochem. Bioph. Res. Commun.* **2000**, *275*, 20–25.
- 344 (14) Bhat, V. B.; Madyastha, K. M. Scavenging of peroxynitrite by phycoyanin and phycoyanobilin
345 from *Spirulina platensis*: protection against oxidative damage to DNA. *Biochem. Bioph. Res. Commun.*
346 **2001**, *285*, 262–266.
- 347 (15) Romay, C.; Gonzalez, R. Phycoyanin is an antioxidant protector of human erythrocytes against lysis
348 by peroxy radicals. *J. Pharm. Pharmacol.* **2000**, *52*, 367–368.
- 349 (16) Romay, C.; Armesto, J.; Ramirez, D.; Gonzalez, R.; Ledon, N.; Garcia, I. Antioxidant and anti-
350 inflammatory properties of C-phycoyanin from blue-green algae. *Inflamm. Res.* **1998**, *47*, 36–41.
- 351 (17) Reddy, C.M.; Bhat, V.B.; Kiranmai, G.; Reddy, M.N.; Reddanna, P.; Madyastha, K.M. Selective
352 inhibition of cyclooxygenase-2 by C-phycoyanin, a biliprotein from *Spirulina platensis*. *Biochem.*
353 *Bioph. Res. Commun.* **2000**, *277*, 599–603.
- 354 (18) Torres, A.; Enk, C. D.; Hochberg, M.; Srebnik, M. Porphyrin-334, a potential natural source for UVA
355 protective sunscreens. *Photochem. Photobiol. Sci.* **2006**, *5*, 432–435.
- 356 (19) Scoglio, S.; Canestrari, F.; Benedetti, S.; Benedetti, Y.; Delgado-Esteban, M. Aphanizomenon flos
357 aquae preparation, extracts and purified components thereof for the treatment of neurological,
358 neurodegenerative and mood disorders. *WO 2008000430* **2008**, A2.
- 359 (20) Choi, Y-H.; Yang, D. J.; Kulkarni, A.; Moh, S. H.; Kim, K. W. Mycosporine-Like Amino Acids
360 Promote Wound Healing through Focal Adhesion Kinase (FAK) and Mitogen-Activated Protein Kinases
361 (MAP Kinases) Signaling Pathway in Keratinocytes. *Mar. Drugs* **2015**, *13*, 7055–7066.
- 362 (21) Abd El-Baky, H. H.; El Baz, F. K.; El-Baroty G. S. Characterization of nutraceutical compounds in
363 blue green alga *Spirulina maxima*. *J. Med. Plants Res.* **2008**, *2*, 292–300.

- 364 (22) Benedetti, S.; Rinalducci, S.; Benvenuti, F.; Francogli, S.; Pagliarani, S.; Giorgi, L.; Micheloni, M.;
365 D'Amici, G.M.; Zolla, L.; Canestrari, F. Purification and characterization of phycocyanin from the blue-
366 green alga *Aphanizomenon flos-aquae*. *J. Chromatogr. B: Anal. Technol. Biomed. Life Sci.* **2006**, *833*,
367 12–18.
- 368 (23) Evans, A. M.; Li, D.; Jones, A.; Games, M. P.; Games, D. E.; Gallon, J. R.; Walton, T. J. Analysis by
369 gas chromatography-mass spectrometry of the fatty acid composition during temperature adaptation in
370 *Aphanizomenon flos-aquae*, a diazotrophic cyanobacterium from the Baltic Sea. *Biochem. Soc. Trans.*
371 **1996**, *24*, 475S.
- 372 (24) Abd El-Bakya, H. H.; El-Baroty, G. S. Characterization and bioactivity of phycocyanin isolated from
373 *Spirulina maxima* grown under salt stress *Food Function* **2012**, *3*, 381–388.
- 374 (25) Mendiola, J. A.; Marn, F. R.; Hernandez, F. S.; Arredondo O. B.; Seorns F. J.; Ibaez, E.; Reglero, G.
375 Characterization via liquid chromatography coupled to diode array detector and tandem mass
376 spectrometry of supercritical fluid antioxidant extracts of *Spirulina platensis* microalga. *J. Sep. Sci.*
377 **2005**, *28*, 1031–1038.
- 378 (26) Mucci, A.; Parenti, F.; Righi, V.; Schenetti, L. Citron and Lemon under the lens of HR-MAS NMR
379 spectroscopy. *Food Chem.* **2013**, *141*, 3167–3176.
- 380 (27) Righi, V.; Parenti, F.; Tugnoli, V.; Schenetti, L.; Mucci, A. Crocus sativus Petals: Waste or Valuable
381 Resource? The Answer of High-Resolution and High-Resolution Magic Angle Spinning Nuclear
382 Magnetic Resonance. *J. Agric. Food Chem.* **2015**, *63*, 8439–8444.
- 383 (28) Neuhaus, D.; Williamson, M.P. The Nuclear Overhauser Effect in Structural and Conformational
384 Analysis. 2nd Edition, Wiley-VCH: New York, **2000**.
- 385 (29) Klisch, M.; Richter, P.; Puchta, R.; Donat-P. Häder, D-P.; Bauer, W. The Stereostructure of Porphyrin-
386 334: An Experimental and Computational NMR Investigation. Evidence for an Efficient ‘Proton
387 Sponge’. *Helv. Chim. Acta* **2007**, *90*, 488-511.
- 388 (30) Carignan, M. O.; Carreto, J. I. Characterization Of Mycosporine-Serine-Glycine Methyl Ester, A
389 Major Mycosporine-Like Amino Acid From Dinoflagellates: A Mass Spectrometry Study. *J. Phycol.*
390 **2013**, *49*, 680–688.

- 391 (31) Broberg, A.; Kenne, L. Use of High-Resolution Magic Angle Spinning Nuclear Magnetic Resonance
392 Spectroscopy for in Situ Studies of Low-Molecular-Mass Compounds in Red Algae. *Anal. Biochem.*
393 **2000**, *284*, 367–374.
- 394 (32) Zhang, J.; Li, C.; Yu, G.; Guan, H. Total Synthesis and Structure-Activity Relationship of
395 Glycoglycerolipids from Marine Organisms. *Mar. Drugs* **2014**, *12*, 3634–3659.
- 396 (33) Zou, Y.; Li, Y.; Kim, M-M.; Lee, S-H.; Kim, S-H. Ishigoside, a New Glyceroglycolipid Isolated from
397 the Brown Alga *Ishige okamurae*. *Biotechnol. Bioprocess Eng.* **2009**, *14*, 20–26.
- 398 (34) Groll, M.; Schellenberg, B.; Bachmann, A. S.; Archer, C. R.; Huber, R.; Powell, T. K.; Lindow, S.;
399 Kaiser, M.; Dudler, R. A plant pathogen virulence factor inhibits the eukaryotic proteasome by a novel
400 mechanism. *Nature* **2008**, *452*, 755–758.
- 401 (35) Groll, M.; Berkers, C. R.; Ploegh, H. L.; Ovaa, H. Crystal structure of the boronic acid-based
402 proteasome inhibitor bortezomib in complex with the yeast 20S proteasome. *Structure* **2006**, *14*, 451–
403 456.
- 404 (36) Roullier, C.; Chollet-Krugler, M.; Pferschy-Wenzig, E-M.; Maillard, A.; Rechberger, G. N.; Legouin-
405 Gargadennec, B.; Bauer, R.; Boustie, J. Characterization and identification of mycosporines-like
406 compounds in cyanolichens. Isolation of mycosporine hydroxyglutamicol from *Nephroma laevigatum*
407 *Ach. Phytochem.* **2011**, *72*, 1348–1357.
- 408 (37) Chen, J.; Song, D.; Luo, Q.; Mou, T.; Yang, R.; Chen, H.; He, S.; Yan X. Determination of
409 Floridoside and Isofloridoside in Red Algae by High-Performance Liquid Chromatography Tandem
410 Mass Spectrometry, *Anal. Lett.* **2014**, *47*, 2307–2316.
- 411 (38) Drews, G.; Meyer, H. Chemical composition of cell walls of *Anacystis nidulans* and *Chlorogloea*
412 *fritschii*. *Arch. Microbiol.* **1964**, *48*, 259–267.

413

414

415

416 **FIGURE CAPTIONS**

417

418 **Scheme 1.** Structures of porphyrin-334 (P334), shinorine (Shi), glyceryl β -D-galactopyranoside (GalpG), *cis*-
419 3,4-dehydrolysine (DhLys) and glyceryl 6-amino-6-deoxy- α -D-glucopyranoside (ADG).

420 **Fig. 1.** Water-saturated ^1H NMR spectrum of Klamath algae suspension in D_2O . * residual HDO signal.
421 Interesting metabolites are labelled: porphyrin-334 (P334), shinorine (Shi), glyceryl β -D-galactopyranoside
422 (GalpG), *cis*-3,4-dehydrolysine (DhLys), glyceryl 6-amino-6-deoxy- α -D-glucopyranoside (ADG), alanine
423 and bound forms of alanine (Ala, Ala- and -Ala), acetate (Ac), *N*-acetyls (*N*-Ac), lactate (Lac), aspartate
424 (Asp), threonine (Thr).

425 **Fig. 2.** Partial HSQC spectrum of Klamath algae suspension in D_2O evidencing signals of P334, Shi (ovals)
426 and GalpG (rectangles).

427 **Fig. 3.** Partial ROESY spectrum of Klamath algae suspension in D_2O evidencing signals of P334 and Shi.

428 **Fig. 4.** Partial TOCSY spectrum of Klamath algae suspension in D_2O evidencing signals of DhLys
429 (left) and ADG (right)

430

431 **Table 1.** NMR data (600 MHz, D₂O) for selected metabolites found in AFA^a

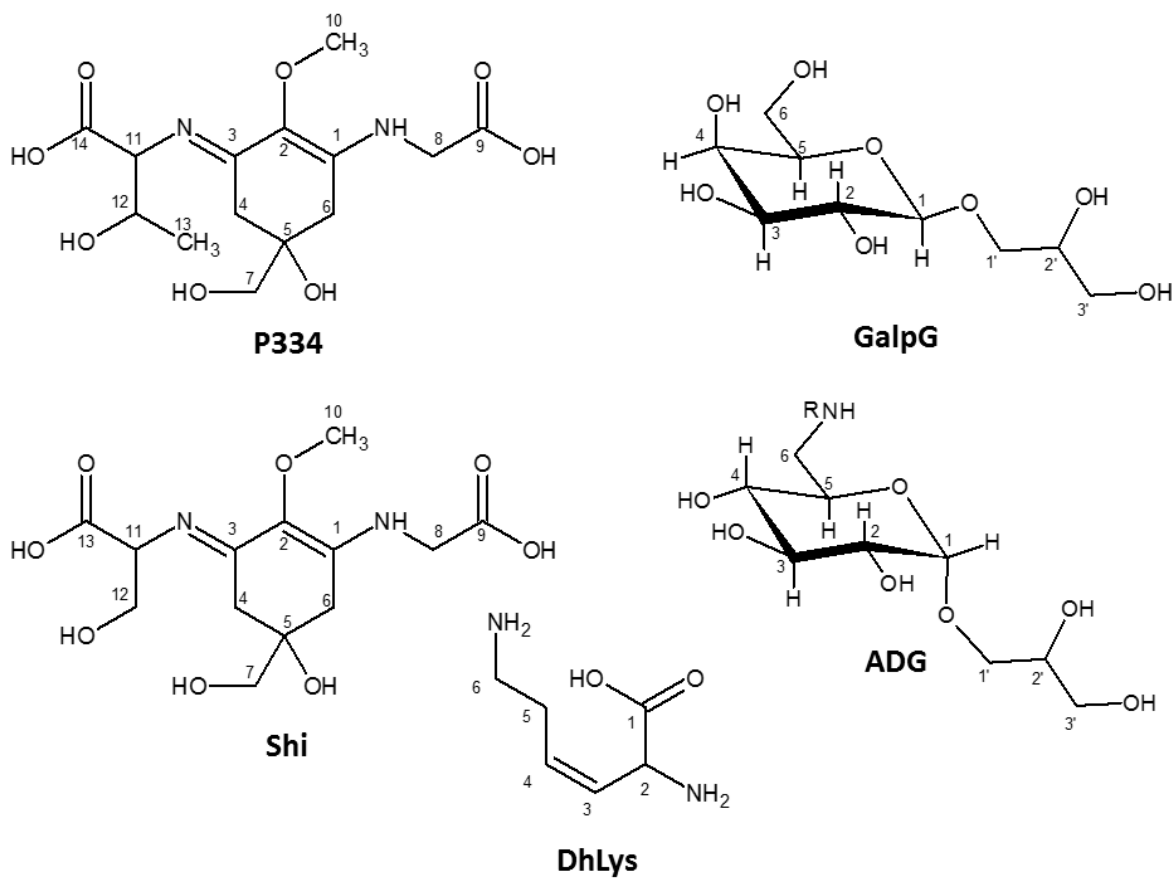
Metabolite	nuclei	H (δ, ppm, J, Hz)	C (δ, ppm)	Note ^b
P334	CH ₂ -8	4.03	49.5	HMBC 163.3 (C1), 177.7(C9), COSY, TOCSY 8.6 (NH)
	CH ₂ -6	2.75 (d, J = 17.3), 2.82 (d, J = 17.3)	35.8	HMBC 163.3(C1), ROESY 4.03
	CH ₂ -7	3.57	70.4	HMBC 35.8, 36.1, 73.8 (C5)
	CH ₂ -4	2.89 (d, J = 17.3), 2.74 (d, J = 17.3)	36.1	HMBC 161.8 (C3), 73.8 (C5), 128.5 (C2) ROESY with 4.06
	CH ₃ -10	3.69	62.2	HMBC 128.5 (C2)
	CH-11	4.06	67.3	HMBC 178.2 (C14), 161.8 (C3), TOCSY 7.63 (NH)
	CH ₃ -13	1.25 (d, 6.3)	22.2	HMBC 67.3, 71.0 NOESY 2.89 TOCSY 7.63 (NH)
	CH-12	4.30	71.0	COSY 1.25, 4.06
Shi serine residue	CH ₂ -4	2.92 (d, J = 17.2), 2.77 (d, J = 17.2)	36.1	ROESY 3.57 , 4.34
	CH-11	4.34	63.3	HMBC 177.5 (C13), 161.9 (C3) COSY 3.92, 3.99
	CH ₂ -12	3.92 (t), 3.99 (d)	65.3	HMBC 177.5 (C13)
GalpG	CH-1	4.40 (d, J=8 Hz)	105.9	ROESY 3.54, 3.65, 3.68 3.76, 3.91
	CH-2	3.55	73.7	HMBC 105.9, 75.5
	CH-3	3.65	75.5	HMBC 73.6
	CH-4	3.92	71.5	HMBC 78.0, 73.6, 75.5, 63.8
	CH-5	3.69	78.0	HMBC 63.8, 71.5
	CH ₂ -6	3.76, 3.79	63.8	HMBC 78.0
	CH ₂ -1'	3.76, 3.91	73.7	HMBC 105.9, 65.3
	CH-2'	3.93	73.2	HMBC 73.7
	CH ₂ -3'	3.60, 3.66	65.3	HMBC 73.7
ADG	CH-1	4.89 (d, 3.6)	101.1	HMBC: 70.9, 71.7, 75.9 COSY 3.58, TOCSY 3.07, 3.38, 3.26, 3.58, 3.75, 4.06 ROESY 3.45, 3.58.

	CH-2	3.58	74.4	
	CH-3	3.73 (t)	75.7	
	CH-4	3.26 (t, 13)	75.4	HMBC 54.9, 70.9, 75.7
	CH-5	4.05 (t, 10)	70.9	
	NCH ₂ -6	3.07 (dd, 9.7,14.7), 3.38 (t, 14.7)	54.9	HMBC 70.9, 75.4
	CH ₂ -1'	3.45 (t), 3.94 (d)	71.7	HMBC 65.5, 73.6, 101.1 TOCSY 3.69, 3.59, 3.94 ROESY 3.45, 3.94
	CH-2'	nd	73.6	
	CH ₂ -3'	3.69, 3.59	65.5	
cis-3,4-DhLys	CH-2	4.59 (d, 9.8 Hz)	54.7	HMBC 128.1, 135.1, 175.6 ROESY 2.66, 2.58
	CH-3	5.66 (t, 10.2 Hz)	128.1	
	CH-4	5.88(m)	135.1	
	CH ₂ -5	2.58,2.66	28.2	HMBC 135.1, 128.1, 41.3
	CH ₂ -6	3.13,3.19	41.3	HMBC 135.1, 28.2

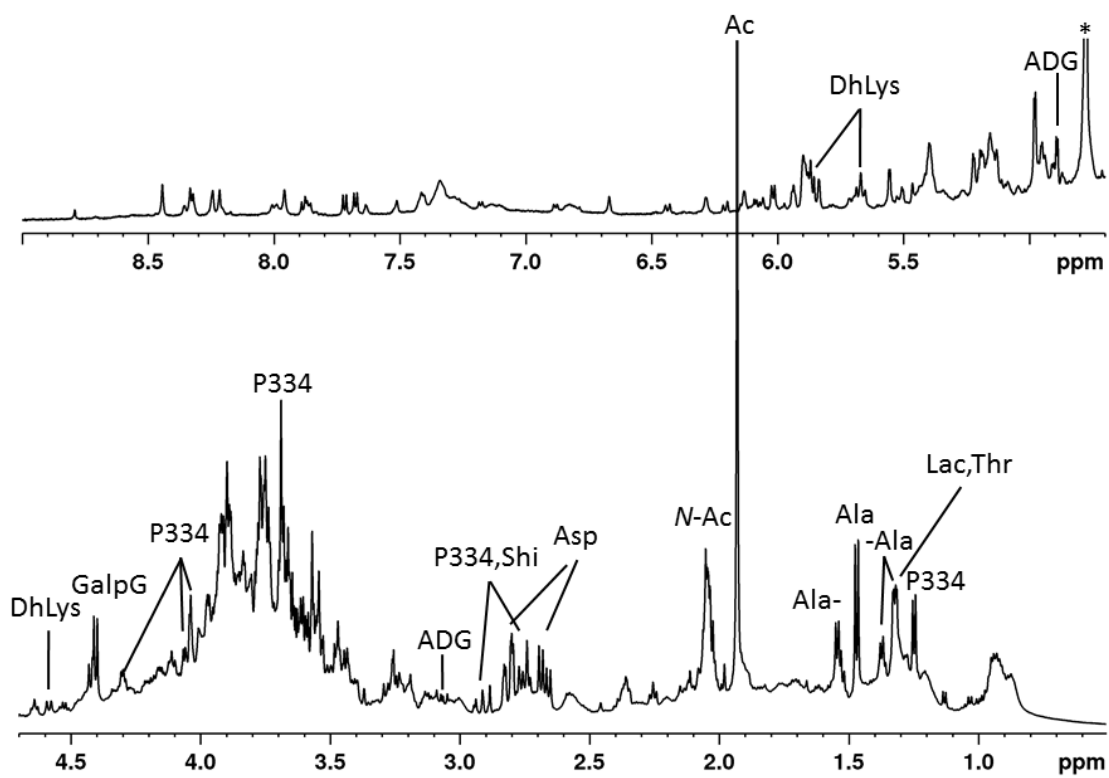
432 ^a Ala CH₃ signal (at 1.47 and 19.0 ppm, for proton and carbon, respectively, see Table S1) was used as
 433 internal reference for ¹H and ¹³C chemical shifts.

434 ^b Relevant correlations observed in 2D spectra: HMBC, TOCSY, COSY, ROESY, NOESY.

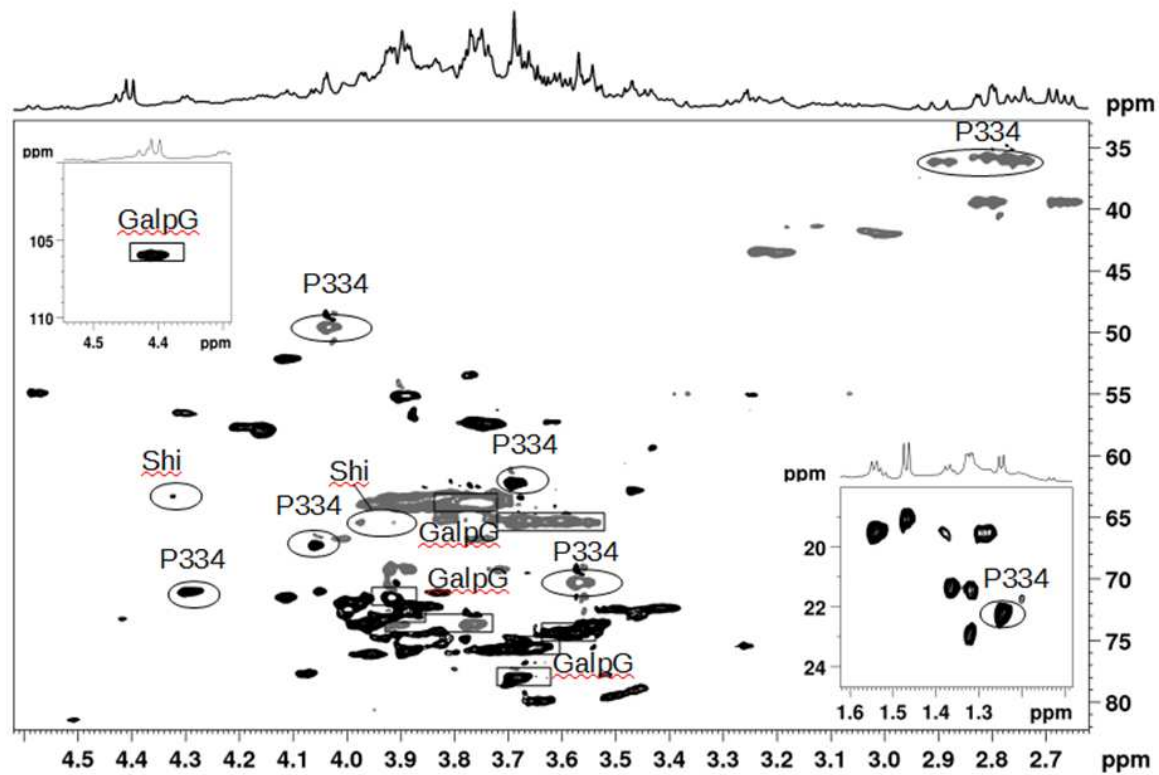
435



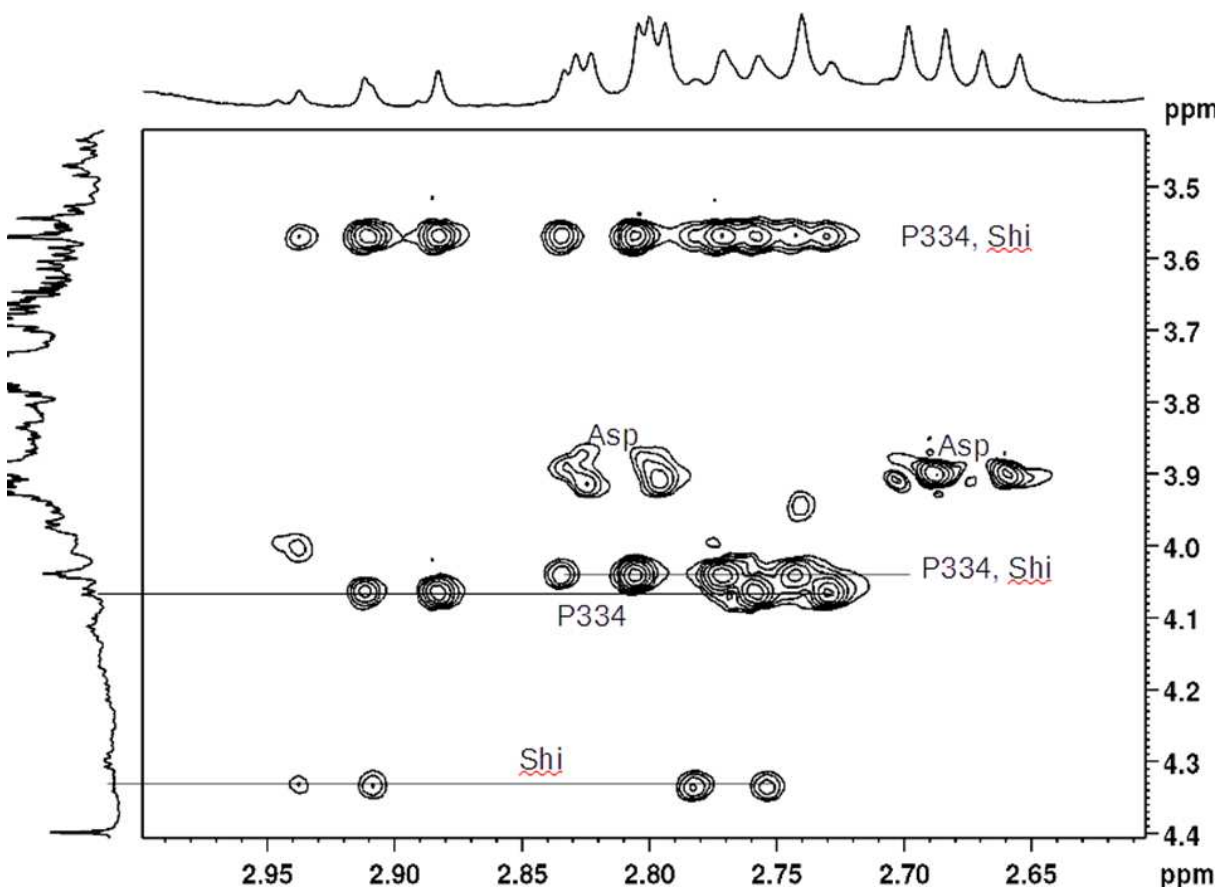
436
437 Scheme 1



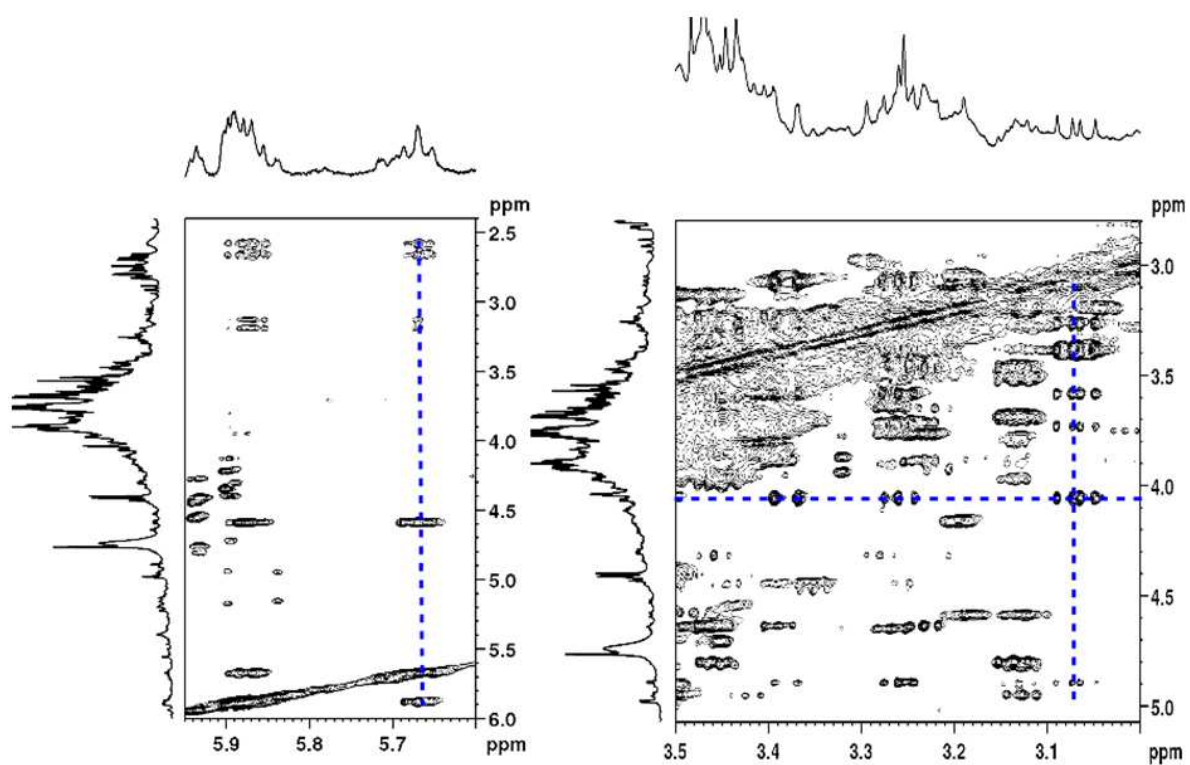
438
439 Figure 1



440
441 Figure 2



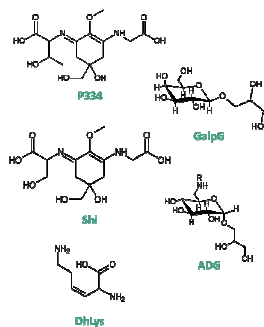
442
443 Figure 3



444
445 Figure 4
446

447 GRAPHIC FOR TOC

448



449

450